

Multiphoton Sub-Band-Gap Photoconductivity and Critical Transition Temperature in Type-II GaSb Quantum-Dot Intermediate-Band Solar Cells

Jinyoung Hwang, Kyusang Lee, Alan Teran, Stephen Forrest, and Jamie D. Phillips*

*Department of Electrical Engineering and Computer Science, University of Michigan,
Ann Arbor, Michigan 48109, USA*

Andrew J. Martin and Joanna Millunchick

*Department of Materials Science and Engineering, University of Michigan,
Ann Arbor, Michigan 48109, USA*

(Received 3 April 2014; published 26 June 2014)

Multiphoton transitions in GaSb/GaAs quantum-dot intermediate-band solar cells are investigated at variable temperature and excitation intensity. A transition temperature is observed that corresponds to the crossover between quantum-dot intraband transitions dominated by thermal escape due to infrared photogeneration. The transition temperature follows an Arrhenius relation with an activation energy of 220 meV that corresponds to the energy barrier observed by holes in the quantum dots. The transition temperature is in the range of 160–225 K for the temperature range studied, significantly higher than observed in previous type-I quantum-dot systems. These results illustrate the potential of type-II structures with deep confinement potentials and strong intraband absorption for future intermediate-band solar cells and quantum devices.

DOI: 10.1103/PhysRevApplied.1.051003

Solar-energy conversion via intermediate-electronic states in the band gap of a semiconductor provides an opportunity to enhance energy conversion by increasing current generation, while maintaining a voltage that tracks the band gap of the semiconductor. The intermediate-band solar cell (IBSC) approach, considered decades ago by Wolf [1] and motivated in 1997 by Luque and Martí [2], has spurred research to identify appropriate materials as described in several recent reviews [3–5]. Enhancements in current generation are realized in quantum dots [6,7], quantum wells [8], and bulk materials [9] due to enhanced sub-band-gap response. However, efficiency also relies on the ability to achieve a quasi-Fermi-level splitting that exceeds the energy associated with the intermediate band in order to preserve the desired voltage of the solar cell [10]. The common source for voltage reduction in an IBSC is thermal escape of carriers relative to the rate of optically induced sub-band-gap transitions [11,12]. Thus far, experiments to demonstrate the proper operation of the intermediate-band solar cell have required solar concentration to enhance sub-band-gap optical generation rates or operation below room temperature to reduce thermal-carrier escape rates [8,11,13]. Among the IBSC approaches utilizing quantum-confined structures, type-II band alignments are proposed with expectations of enhanced absorption, more favorable energetic positioning, or reduced thermal-carrier escape rates [14–18]. Type-II GaSb/GaAs quantum dots (QDs) have demonstrated sub-band-gap intermediate-band

solar-energy conversion and properties that are promising for enhanced performance relative to type-I structures [15,19–25].

A common technique used to illustrate sub-band-gap response in IBSCs is through external quantum-efficiency spectra. However, since these measurements are typically performed under monochromatic illumination, they do not accurately describe the behavior of sub-band-gap energy-conversion processes via intermediate-band states. Experiments utilizing multiple sub-band-gap sources provide a more appropriate measure of intermediate-band response, with sequential photogeneration across intermediate-electronic states. This technique has been referred to as two-photon sub-band-gap photocurrent (TPPC) [5], with several variations on how to conduct the experiments. In this work, the temperature and illumination-intensity-dependent TPPC are studied in type-II GaSb/GaAs QDs. The conditions where intraband transitions transition from optical to thermal-carrier escape are evaluated.

Solar cells with ten layers of GaSb QDs are studied with materials-growth and device-fabrication procedures reported previously [22,26]. Spectral measurements of the external quantum efficiency (EQE) are performed using a broadband source, a monochromator, a lock-in amplifier, and comparison with a calibrated detector. Two-photon measurements are conducted by continuous illumination by a monochromatic light source as an initial pump to excite holes into the GaSb quantum dots, and an additional IR source via a chopped 1550-nm laser with a nominal power of 20 mW, as shown in Fig. 1. The two-photon technique is

*jphilli@umich.edu

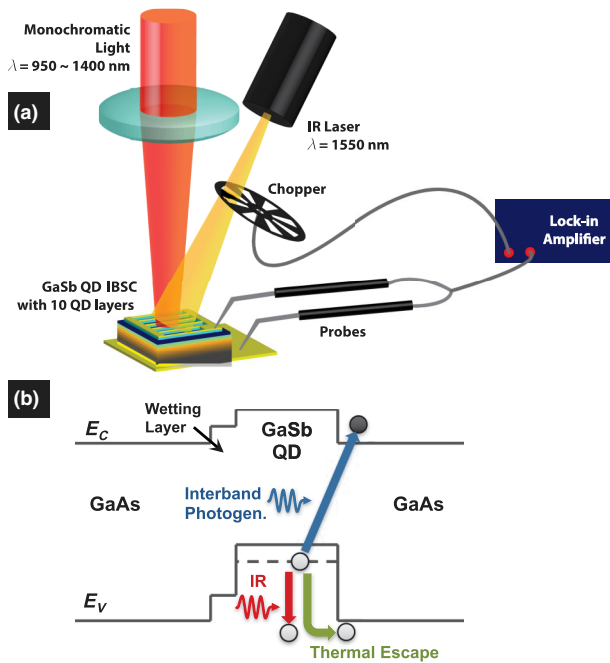


FIG. 1. Schematic drawing of (a) a measurement setup for multiphoton quantum-efficiency measurements using a chopped IR source and (b) an energy-band diagram for the GaSb/GaAs QD system illustrating optically induced interband transitions, optical generation via additional IR illumination, and thermal-hole escape from confined states in the QDs.

referred to as the TPPC1 experiment from Ramiro *et al.* [5]. Temperature-dependent measurements are conducted using a closed-cycle cryostat, and variable IR intensity is introduced using variable focus and neutral-density filters.

The electrical characteristics and response under AM1.5 illumination have been previously reported [22], with nominal power-conversion efficiencies of 12.5% and 18% under AM1.5 illumination for GaSb/GaAs QD cells and GaAs reference cells, respectively. Single-photon EQE measurements at room temperature are shown in Fig. 2 comparing the QD solar cell to a reference GaAs solar cell. Reduced EQE is observed for the GaSb/GaAs QD cell in the spectral region just above the band gap, and is consistent with the reduced power-conversion efficiency. The reduced EQE in this region may be due to recombination via the QDs or via nonradiative recombination associated with defects introduced by the QDs [6,25]. The reduced EQE also correlates with a reduced cell voltage [22], and due to the nonideal behavior, prevents the ability to draw direct correlations between cell voltage and QD behavior. Further development of cell design, such as the inclusion of strain-compensating layers [6], is ultimately expected to reduce the observed nonidealities.

Alternatively, the sub-band-gap response of the QD cells can reveal information on key electronic transitions. An enhanced response is observed below the GaAs band edge in the range of 900–1240 nm. The sub-band-gap response

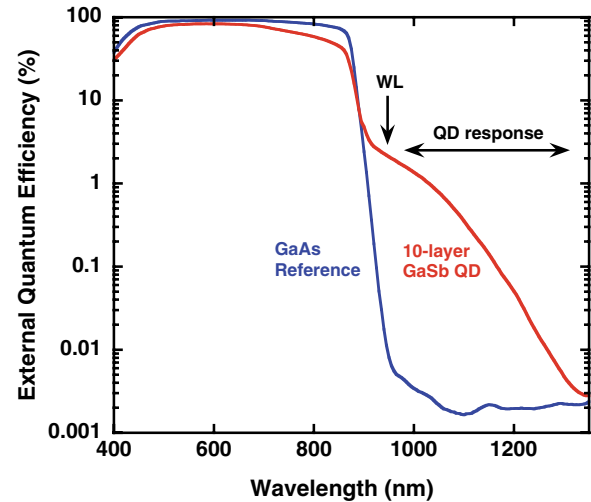


FIG. 2. Room-temperature external-quantum efficiency of a 10-layer GaSb/GaAs QD solar cell and comparison to a GaAs reference cell. Sub-band-gap photoresponse is observed in a spectral range consistent with interband optical transitions in the GaSb quantum dots and wetting layer.

corresponds to transitions previously established from a combination of low-temperature photoluminescence measurements and eight-band $k \cdot p$ calculations [26]. These transitions are labeled in Fig. 2 as the GaSb wetting layer (WL) at 1.36 eV (912 nm) and GaSb quantum dots in the range of 1.00–1.26 eV (1240–984 nm). The observation of sub-band-gap current response is a result of interband photexcitation between the GaAs conduction band and the confined states of the GaSb quantum dots. In the absence of additional IR illumination, photoresponse is achieved via thermal-carrier escape.

Variable-temperature TPPC1 experiments conducted as a function of wavelength of the pump beam are shown in Fig. 3. The response reveals photocurrent generated via sub-band-gap transitions, where the pump beam excites holes into confined states in the GaSb QDs. The chopped IR illumination further excites holes from the GaSb QDs to the GaAs valence band to generate a photocurrent. The photocurrent response decays for wavelengths longer than 1200 nm, where the energy of the pump beam is insufficient to generate holes in the GaSb QDs. For temperatures of approximately 250 K and above, thermal-carrier escape is dominant and IR illumination does not impact sub-band-gap photocurrent generation.

The temperature dependence of photocurrent generation under chopped IR illumination is also shown in Fig. 4 for a fixed-pump wavelength of 1000 nm. The sub-band-gap photocurrent is nearly constant at low temperatures, and decreases rapidly at a temperature where thermal-carrier escape matches and then exceeds the optical generation rate provided by the chopped IR illumination. The transition temperature is defined in this work as the 50% point of the maximum sub-band-gap photocurrent. The

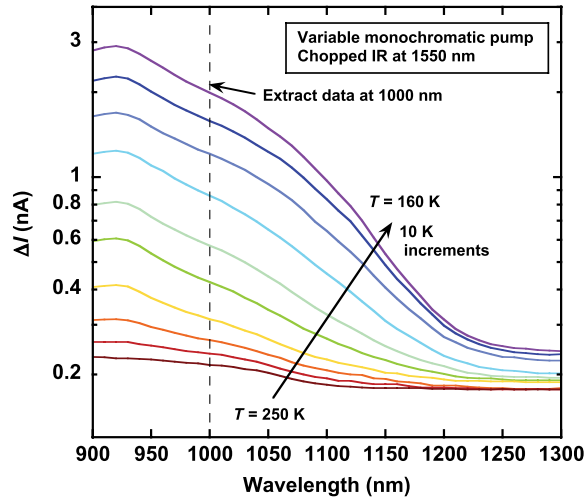


FIG. 3. Two-photon sub-band-gap photocurrent response due to chopped IR illumination at 1550 nm and steady-state monochromatic illumination at variable wavelength. An increased response is observed at reduced temperature due to reduced-carrier thermal escape.

temperature-dependent response in Fig. 4 is shown for several IR-illumination intensities, where the transition temperature increases with increasing IR power. This behavior is consistent with increased intraband-optical generation, and the allowance for higher temperatures before thermal-carrier escape becomes dominant. The intensity dependence of the photocurrent produced by IR illumination is nonlinear, which may result from the saturation of QD states and/or carrier-density dependence of nonradiative and radiative generation-recombination processes.

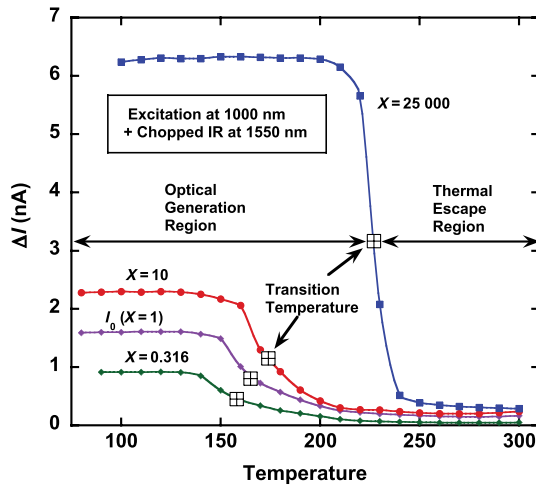


FIG. 4. Two-photon sub-band-gap photocurrent response versus temperature for several cases of chopped IR-illumination intensity at 1550 nm and steady-state illumination at 1000 nm. A transition temperature is observed corresponding to the cross-over from intraband transitions due to IR photogeneration to thermal-hole escape.

The optical generation rate G_{opt} and thermal-carrier escape rate G_{th} are given by

$$G_{\text{opt}} = \sigma_{\text{opt}}\phi, \quad (1)$$

$$G_{\text{th}} = \sigma_{\text{th}}\gamma T^2 \exp(-E_A/k_B T), \quad (2)$$

where σ_{opt} and σ_{th} are the cross sections for optical and thermal processes, respectively, ϕ is the photon flux, γ is the temperature-independent emission-rate parameter, E_A is the activation energy of the transition, and k_B is the Boltzmann constant. The transition temperature T_{tr} where optical and thermal generation rates are equal results in the expression

$$\sigma_{\text{opt}}\phi = \sigma_{\text{th}}\gamma T_{\text{tr}}^2 \exp(-E_A/k_B T_{\text{tr}}). \quad (3)$$

The transition point follows an Arrhenius relation:

$$\ln\left(\frac{X}{T_{\text{tr}}^2}\right) = \ln\left(\frac{E}{I_0} \frac{\sigma_{\text{th}}}{\sigma_{\text{opt}}} \gamma\right) - \frac{E_A}{k_B T_{\text{tr}}}, \quad (4)$$

where the IR photon flux is given by $\phi = XI_0/E$, I_0 is a baseline intensity of the IR source, E is the energy of the IR source, and X is a multiplier for the IR source for variable-intensity measurements. The baseline intensity of the source for these experiments is $I_0 = 30 \text{ mW/cm}^2$. For a given material or device, the activation energy may be extracted by determining the transition temperature T_{tr} vs X . The transition temperatures in Fig. 4 are plotted in Arrhenius form in Fig. 5. The extracted activation energy of 220 meV is consistent with the barrier height for confined holes in the GaSb QDs [15].

The transition temperature effectively defines the temperature where the solar cell can be operated for a given infrared intensity (or corresponding solar concentration

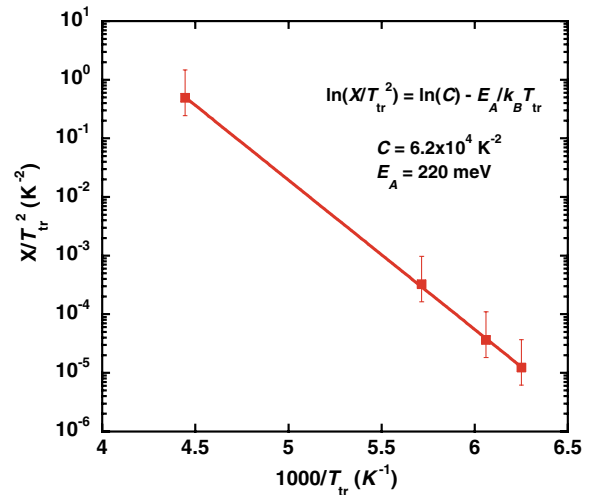


FIG. 5. Plot relating the transition temperature for varying IR intensity resulting in an activation energy of 220 meV.

after accounting for the intraband absorption spectrum), to ensure that optical generation is dominant. This is a fundamental requirement to ensure that the open-circuit voltage is not significantly reduced by the low-band-gap quantum dot. The range of transition temperatures of 160–225 K observed for the GaSb QDs is promising, where much lower temperatures (approximately 50 K and below [11]) were required in previous type-I InAs/GaAs QDs. The increased transition temperature is likely due to a combination of both increased intraband-optical absorption (higher σ_{opt}) for the GaSb QDs, and reduced thermal escape due to the increased confinement potential, as described previously [15].

The transition temperature will have a strong dependence on the absolute intensity of the IR source. The baseline intensity of $I_0 = 30 \text{ mW/cm}^2$ for the 1550-nm source corresponds to a photon flux of 2.2×10^{21} photons/ $\text{m}^2 \text{ s}$. In comparison, the photon flux for AM1.5 solar illumination in the 0.2–1.0 eV spectral window that is accessible for intraband transitions in the GaSb quantum dots provides a photon flux of 2.4×10^{21} photons/ $\text{m}^2 \text{ s}$. The $X = 1$ condition in this study therefore corresponds to approximately one sun illumination for the accessible spectral window for intraband transitions. The use of a monochromatic source in these experiments, however, does not provide a direct comparison to broadband solar illumination since the absorption spectrum of the QDs exhibit a narrow spectral band centered near the energy of the confinement potential. The optical absorption for intraband transitions in quantum dots [27], described by σ_{opt} , is expected to be much weaker for 1550 nm illumination (0.8 eV) than longer wavelength photons in the broadband solar spectrum that are nearer the 0.22 eV activation energy associated with the quantum dots. The transition temperature under AM1.5 conditions would therefore be expected to be higher than the measured value of 165 K for a similar flux at 1550 nm.

Further quantitative understanding of intermediate-band solar-energy conversion in GaSb QDs requires a more detailed understanding of intraband-optical processes. The significant improvement in transition temperature observed in this system motivates further efforts for band-structure engineering to achieve strong optical-absorption transitions and to approaches such as energy fence barriers [10] to reduce thermal-escape processes. Furthermore, the two-photon experiments and analysis of transition temperatures described here provide an effective method of validating sub-band-gap response and determining temperature and illumination conditions where intermediate-band solar-energy conversion may operate with enhanced power-conversion efficiency. In addition, the measurement and observed reduction of thermal-carrier escape in type-II quantum dots may further impact applications including inter-sub-band detectors and sources and devices for quantum information processing.

This work was supported as part of the Center for Solar and Thermal Energy Conversion, an Energy Frontier Research Center funded by the U.S. Department of Energy, Office of Science, Office of Basic Energy Sciences under Award No. DE-SC0000957.

-
- [1] M. Wolf, Limitations and possibilities for improvement of photovoltaic solar energy converters: Part I: Considerations for Earth's surface operation, *Proc. IRE* **48**, 1246 (1960).
 - [2] A. Luque and A. Marti, Increasing the efficiency of ideal solar cells by photon induced transitions at intermediate levels, *Phys. Rev. Lett.* **78**, 5014 (1997).
 - [3] A. Luque, P. G. Linares, E. Antolin, I. Ramiro, C. D. Farmer, E. Hernandez, I. Tobias, C. R. Stanley, and A. Marti, Understanding the operation of quantum dot intermediate band solar cells, *J. Appl. Phys.* **111**, 044502 (2012).
 - [4] Y. Okada, K. Yoshida, Y. Shoji, and T. Sogabe, Recent progress on quantum dot intermediate band solar cells, *IEICE Electron. Express* **10**, 20132007 (2013).
 - [5] I. Ramiro, A. Marti, E. Antolin, and A. Luque, Review of experimental results related to the operation of intermediate band solar cells, *IEEE J. Photovoltaics* **4**, 736 (2014).
 - [6] S. M. Hubbard, C. D. Cress, C. G. Bailey, R. P. Raffaele, S. G. Bailey, and D. M. Wilt, Effect of strain compensation on quantum dot enhanced GaAs solar cells, *Appl. Phys. Lett.* **92**, 123512 (2008).
 - [7] R. B. Laghumavarapu, A. Moscho, A. Khoshakhlagh, M. El-Emawy, L. F. Lester, and D. L. Huffaker, GaSb/GaAs type II quantum dot solar cells for enhanced infrared spectral response, *Appl. Phys. Lett.* **90**, 173125 (2007).
 - [8] S. Masakazu, W. Yunpeng, F. Hiromasa, S. Hassanet, W. Kentaroh, and N. Yoshiaki, A quantum-well superlattice solar cell for enhanced current output and minimized drop in open-circuit voltage under sunlight concentration, *J. Phys. D* **46**, 024001 (2013).
 - [9] W. Weiming, A. S. Lin, and J. D. Phillips, Intermediate-band photovoltaic solar cell based on ZnTe:O, *Appl. Phys. Lett.* **95**, 011103 (2009).
 - [10] G. Wei, K.-T. Shiu, N. C. Giebink, and S. R. Forrest, Thermodynamic limits of quantum photovoltaic cell efficiency, *Appl. Phys. Lett.* **91**, 223507 (2007).
 - [11] E. Antolin, A. Marti, C. R. Stanley, C. D. Farmer, E. Canovas, N. Lopez, P. G. Linares, and A. Luque, Low temperature characterization of the photocurrent produced by two-photon transitions in a quantum dot intermediate band solar cell, *Thin Solid Films* **516**, 6919 (2008).
 - [12] E. Antolin, A. Marti, C. D. Farmer, P. G. Linares, E. Hernandez, A. M. Sanchez, T. Ben, S. I. Molina, C. R. Stanley, and A. Luque, Reducing carrier escape in the InAs/GaAs quantum dot intermediate band solar cell, *J. Appl. Phys.* **108**, 064513 (2010).
 - [13] P. G. Linares, A. Marti, E. Antolin, I. Ramiro, E. Lopez, E. Hernandez, D. Fuertes Marron, I. Artacho, I. Tobias, P. Gerard, C. Chaix, R. P. Campion, C. T. Foxon, C. R. Stanley, S. I. Molina, and A. Luque, Extreme voltage recovery in GaAs:Ti intermediate band solar cells, *Sol. Energy Mater. Sol. Cells* **108**, 175 (2013).

- [14] L. Cuadra, A. Martí, and A. Luque, Type II broken band heterostructure quantum dot to obtain a material for the intermediate band solar cell, *Physica (Amsterdam)* **14E**, 162 (2002).
- [15] H. Jinyoung, A. J. Martin, J. M. Millunchick, and J. D. Phillips, Thermal emission in type-II GaSb/GaAs quantum dots and prospects for intermediate band solar energy conversion, *J. Appl. Phys.* **111**, 074514 (2012).
- [16] R. B. Laghumavarapu, B. L. Liang, Z. S. Bittner, T. S. Navruz, S. M. Hubbard, A. Norman, and D. L. Huffaker, GaSb/InGaAs quantum dot-well hybrid structure active regions in solar cells, *Sol. Energy Mater. Sol. Cells* **114**, 165 (2013).
- [17] Hu Weiguo, M. E. Fauzi, M. Igarashi, A. Higo, Lee Ming-Yi, Li Yiming, N. Usami, and S. Samukawa, Type-II Ge/Si quantum dot superlattice for intermediate-band solar cell applications, in *Proceedings of the 2013 IEEE 39th Photovoltaic Specialists Conference (PVSC)* (IEEE, Piscataway, NJ, 2013), p. 1021.
- [18] Antonio Luque, Pablo G. Linares, Alex Mellor, Viacheslav Andreev, and Antonio Martí, Some advantages of intermediate band solar cells based on type II quantum dots, *Appl. Phys. Lett.* **103**, 123901 (2013).
- [19] R. B. Laghumavarapu, A. Moscho, A. Khoshakhlagh, M. El-Emawy, L. F. Lester, and D. L. Huffaker, GaSb/GaAs Type II quantum dot solar cells for enhanced infrared spectral response, *Appl. Phys. Lett.* **90**, 173125 (2007).
- [20] P. J. Carrington, A. S. Mahajumi, M. C. Wagener, J. R. Botha, Zhuang Qian, and A. Krier, Type II GaSb/GaAs quantum dot/ring stacks with extended photoresponse for efficient solar cells, *Physica (Amsterdam)* **407B**, 1493 (2012).
- [21] P. J. Carrington, M. C. Wagener, J. R. Botha, A. M. Sanchez, and A. Krier, Enhanced infrared photo-response from GaSb/GaAs quantum ring solar cells, *Appl. Phys. Lett.* **101**, 231101 (2012).
- [22] J. Hwang, A. J. Martin, L. Kyusang, S. Forrest, J. Millunchick, and J. Phillips, Preserving voltage and long wavelength photoresponse in GaSb/GaAs quantum dot solar cells, in *Proceedings of the 2013 IEEE 39th Photovoltaic Specialists Conference (PVSC)* (Ref. [17]), pp. 3191–3194.
- [23] R. B. Laghumavarapu, B. L. Liang, Z. Bittner, T. S. Navruz, S. M. Hubbard, A. Norman, and D. L. Huffaker, GaSb/InGaAs quantum dot-well solar cells, in *Proceedings of the 2013 IEEE 39th Photovoltaic Specialists Conference (PVSC)* (Ref. [17]), pp. 0292–02925.
- [24] H. Fujita, J. James, P. J. Carrington, A. R. J. Marshall, A. Krier, M. C. Wagener, and J. R. Botha, Carrier extraction behaviour in type II GaSb/GaAs quantum ring solar cells, *Semicond. Sci. Technol.* **29**, 035014 (2014).
- [25] S. Hatch, J. Wu, K. Sablon, P. Lam, M. Tang, Q. Jiang, and H. Liu, InAs/GaAsSb quantum dot solar cells, *Opt. Express* **22**, A679 (2014).
- [26] A. J. Martin, J. Hwang, E. Marquis, E. P. Smakman, T. W. Saucer, G. V. Rodriguez, A. Hunter, V. Sih, P. M. Koenraad, J. D. Phillips, and J. Mirecki Millunchick, The disintegration of GaSb/GaAs nanostructures upon capping, *Appl. Phys. Lett.* **102**, 113103 (2013).
- [27] B. Kochman, A. D. Stiff-Roberts, S. Chakrabarti, J. D. Phillips, S. Krishna, J. Singh, and P. Bhattacharya, Absorption, carrier lifetime, and gain in InAs-GaAs quantum-dot infrared photodetectors, *IEEE J. Quantum Electron.* **39**, 459 (2003).